Journal of Drug Delivery Science and Technology xxx (xxxx) xxx

Contents lists available at ScienceDirect

Journal of Drug Delivery Science and Technology

journal homepage: www.elsevier.com/locate/jddst

Research paper

Metformin and Silibinin co-loaded PLGA-PEG nanoparticles for effective combination therapy against human breast cancer cells

Soumaye Amirsaadat [a,1], Davoud Jafari-Gharabaghlou [b,1], Sepideh Alijani [c], Hanieh Mousazadeh [b], Mehdi Dadashpour [c], Nosratollah Zarghami [a,b,c,*]

[a] Department of Medical Biotechnology, Faculty of Advanced Medical Sciences, Tabriz University of Medical Sciences, Tabriz, Iran
[b] Department of Clinical Biochemistry and Laboratory Medicine, Faculty of Medicine, Tabriz University of Medical Sciences, Tabriz, Iran
[c] Stem Cell Research Center, Tabriz University of Medical Sciences, Tabriz, Iran

ARTICLE INFO

Keywords:
Metformin
Silibinin
Combination therapy
PLGA-PEG nanoparticles
Breast cancer

ABSTRACT

Polymeric nanoparticle (NP) mediated combination chemotherapy has been proposed to be an efficient strategy for cancer treatment via exerting synergism among the different drugs, suppressing drug resistance, and enhancing pharmacokinetics of the drugs which leads to a decrease in the side effects of the drug payloads. The present study examines the synergistic anticancer efficiency of two natural-based anticancer agents, Metformin (MET) and Silibinin (SIL) co-loaded PLGA-PEG NPs against T47D breast cancer cells. The resultant drug-loaded PLGA-PEG NPs displayed a spherical morphology with the uniform nanosize distribution. For both drugs, burst discharge occurred in the first 8 h, followed by sustained release over 7 days. According to MTT assay and median-effect analysis, MET/SIL-loaded PLGA-PEG NPs exhibited the most synergistic cytotoxic effect against the breast cancer cells. Besides, it was revealed that the dual drug-loaded NPs could significantly alter the expression levels of Bax, Bcl-2, caspase 3 and 9, and hTERT compared to the free combination of the drugs as well as the single drug-loaded NPs. Taken together, this work revealed that MET/SIL-loaded PLGA-PEG NP based combination therapy might have a significant potential to improve the efficiency of breast cancer therapy.

1. Introduction

Breast cancer is the more invasive and high incidence cancer between the women in the worldwide, and the survival limit of its 5-years is about 75% [1]. Though some chemotherapy approaches have been improved to remedy this kind of cancer, several concerns such as reoccurrence after radiotherapy and chemotherapy, and low survival rate remains [2]. Therefore, novel strategies and efficient treatment methods must be adopted. The utilization of traditional chemotherapy and radiotherapy treatments are limited because of their detrimental side effects and extra toxicity on the untargeted tissue [3]. Thus, the progress of alternative therapies is an effective approach that might aid to decrease the side effects of breast cancer treatment.

Recent outstanding developments in treating various types of cancer have increasingly passed from mono-chemotherapy to combinatorial chemotherapy, in which multiple chemotherapeutic agents can integrate into a single platform to generate efficient therapeutic outcomes through cooperative interactions among the drugs than individual treatments [4,5].

Besides, interventions with nontoxic phytochemicals evaluated at several studies have shown a decrease in cancer recurrence and improvement of treatment [6]. Hence, developing efficient antitumor therapy with low side effects is crucial and natural-based anti-cancer agents such as Metformin (MET) and Silibinin (SIL) possess significant potential for such treatment approaches.

SIL is the main and active component of silymarin which extracts from milk thistle seeds and has the potential of cancer treatment [7]. Researches recently have described that SIL has anti-tumor, anti-inflammatory, and anti-proliferative features and protective effects against toxicity induced by chemotherapy drugs. SIL-treated prostate and breast cancer cells have shown a decrease in the expression level of telomerase. Furthermore, based on some studies SIL could arrest the proliferation of tumor cells through modulation of the STAT, PI3K/Akt, NF-kB, and MAPK pathways [8].

MET (N′, *N*-dimethyl biguanide) from the biguanide family has been accepted by the FDA as the first-line medication for patients with type 2

* Corresponding author. Department of Clinical Biochemistry and Laboratory Medicine, Faculty of Medicine, Tabriz University of Medical Sciences, Tabriz, Iran.
E-mail address: zarghami@tbzmed.ac.ir (N. Zarghami).
[1] Co-first author.

https://doi.org/10.1016/j.jddst.2020.102107
Received 4 August 2020; Received in revised form 10 September 2020; Accepted 19 September 2020
Available online 28 September 2020

diabetes [9]. Moreover, numerous recent preclinical and clinical studies disclosed that MET can arrest the cell proliferation of various kinds of cancer with the possible mechanism mammalian target of rapamycin (mTOR) modulation [10]. The level of energy in MET-treated cells is low, and leads to AMPK activation, thereby activating the tumor suppressor genes and inhibiting cell proliferation [11].

Notwithstanding the proven capability of MET and SIL in the treatment of cancer, some problems limit their clinical applications [12]. With a positive charge at physiological pH values, MET is a hydrophilic compound and therefore, is partially diffused via lipid membranes. Also, MET exhibits a limited absorption window in the digestive system because of its high-water solubility, thus shows poor bioavailability [13].

SIL has a large and complex structure that reduces its bioavailability and diffusion. On the other hand, insignificant sorption in the gastrointestinal tract, degradation via gastric acid, and low solubility limit its medicinal utilizes [14].

To mitigate these limitations, different nanotechnological approaches are being developed to improve drug bioavailability and reduce the administration of repeated doses. Nanoparticle-based drug delivery approaches possess numerous advantages compared to traditional dosage forms [15].

Polymeric nanoparticle-based drug delivery systems have gained a great deal of research interest in cancer therapy. In comparison with traditional drug delivery systems, the nanoparticulate drug delivery systems show improved effectiveness through enhancing the half-life and stability of chemotherapeutic molecules, enhancing the bioavailability of both hydrophobic and hydrophilic biomolecules as well as allowing targeted and controlled drug release at tumor sites [16–19].

Despite the proven anti-cancer effects of the two natural compounds SIL and MET in several studies in free and nanoformulation form, no study has been performed to investigate the anti-cancer efficacy and nature of the interaction of these two anticancer agents through co-delivering by nanocarriers. Therefore, the purpose of the current work is to design PEGylated PLGA NPs for co-releasing of MET and SIL and assess their *in vitro* combinatorial/synergistic antitumor effectiveness on T47D breast cancer cells.

2. Material and methods

2.1. Cell line and chemicals

T47D human breast cancer cell line (epithelial-like cell line) was obtained from the Cell Bank of Pasteur Institute of Iran (Cat. No C203) and retained as recommended. Metformin (1,1-dimethyl biguanide hydrochloride), Silibinin, dimethyl sulfoxide (3,4,5-Dimethyl thiazol-2-yl)-2,5 diphenyl tetrazolium bromide (MTT), Polyethylene Glycol (PEG, Mw = 4000), stannous octoate ($Sn(Oct)_2$), D, L-lactide (LA), glycolide (GA), DCM (dichloromethane), DMSO (dimethyl sulfoxide), PVA (Polyvinyl alcohol) and methylene chloride were obtained from Sigma-Aldrich (St. Louis, MO, USA). RPMI-1640, Penicillin-Streptomycin, and fetal bovine serum (FBS) were purchased from Gibco BRL; The first Strand of cDNA synthesized with the Kit purchased from Fermentas (Vilnius, Lithuania) and Syber Green PCR Master Mix kit was provided from Roche (Germany).

2.2. Synthesis and characterization of tri-block copolymer PLGA-b-PEG-b-PLGA

The ring-opening polymerization method was used to synthesize the tri-block copolymer PLGA-*b*-PEG-*b*-PLGA [20]. Briefly, LA (2.0 g, 13.9 mmol) and GA (0.6 g, 5.2 mmol), initiator HO-PEG-OH (0.4 g, 0.1 mmol), and $Sn(Oct)_2$ (8 mg, 0.1 mol % of monomers) were added in a glass tube which was connected to a vacuum system. Next, an exhausting-refilling with N_2 process was repeated three times. The tube was sealed and heated to 150 °C in an oil bath for 12 h. After the reaction tube was cooled to room temperature, the resulting copolymers were purified by dissolving them in dichloromethane and then precipitating them into excess methanol. The final product was collected by filtration and vacuum-dried at 40 °C for 24 h. The yield of the reaction was determined by weighing the dried copolymers.

^{1}H NMR (Bruker AC-80) spectroscopy was applied to confirm the structure of the synthesized PLGA-b-PEG-b-PLGA using deuterated chloroform ($CDCl_3$) as a solvent and tetramethylsilane (TMS) as an internal standard. The molecular weight of PLGA-b-PEG-b-PLGA was determined by gel permeation chromatography (GPC, Waters 510 chromatographic instrument, USA) equipped with a refractive index detector. Tetrahydrofuran was applied as an eluting solvent. The GPC data were calibrated with polystyrene with different molecular weights as the standards.

2.3. Preparation and characterization of NPs

MET loaded in PLGA-PEG NPs by the double emulsion (W/O/W) manner with slight modifications. In summary, 200 mg of PLGA-PEG solved in 5 ml of dichloromethane. Thereafter, 20 mg of MET dissolved in 20 ml polyvinyl alcohol (PVA, 1% w/v) was added to the organic phase of the tube and emulsified using ultrasonic (Sonoplus, HD 2070; Bandelin Electronics, Berlin, Germany) with 55% power for 5 min. Eventually, after vacuum evaporation of the dichloromethane (DCM) by a rotary evaporator (Heidolph Instruments, Hei-VAP series) at 40 °C, the MET-NPs were accumulated by centrifugation at 15,000 rpm for 40 min.

SIL-NPs were prepared via the double emulsion (W/O/W) manner. After adding 240 mg of PLGA-PEG in 20 ml of DCM, 20 mg of SIL was added to the mixture and homogenized by a stirrer for 10 min at 27 °C. In the next step, the emulsion and 2 ml of PVA (1% w/v) were emulsified by an ultrasonic probe with 55% power for 5 min thereupon; emulsion leniently pour into 10 ml of PVA and homogenized. After vacuum evaporation of the DCM by a rotary evaporator at 40 °C, the SIL-NPs were accumulated by centrifugation at 15,000 rpm for 40 min and rinsed twice via pure water.

MET/SIL-NPs were also prepared via the enhanced double emulsion (W/O/W) manner. After obtaining the first emulsion, it was homogenized by the stirrer for 2 min at room temperature with 2 ml of PVA (1% w/v). Concurrent, 0.2 ml of SIL-dissolved in DCM was added leniently into a mixture tube and emulsified again for 5 min. The rest of the steps were alike with the production of MET-NPs [21].

A Malvern Instruments Zetasizer Nano-ZS instrument was used for determining the mean size (diameter, nm) and surface charge (ζ-potential, mv) of the NPs. Drug-loaded NPs were prepared by solving the 0.5 mg/ml of NPs in deionized water afterward sonication for 10 min at 27 °C.

Morphology and shape of the gold-coated NPs were scrutinized by a Field emission scanning electron microscopy (FE-SEM) system (Hitachi S-4800, Japan) [22].

IR-spectral information of the pure drugs, MET-NPs, SIL-NPs, and MET/SIL NPs that were prepared in KBr disks was obtained by a PerkinElmer Spectrum One model FTIR spectrometer (from 4000 to 400 cm^{-1}).

To measure the efficiency of drug encapsulation, after the synthesis of drug-loaded NPs, the supernatant of the tube was isolated and the quantity of non-entrapped drugs assessed via an ultraviolet 2550 spectrophotometer (Shimadzu) at the MET and SIL absorbance peak (237 and 288 nm, respectively). In the following, the percent of entrapped drugs (Encapsulation Efficiency; EE) and drug loading (DL) were computed by employing the following formulas:

$$EE = \frac{Weight\ of\ MET\ /\ SIL\ in\ NPs}{Weight\ of\ the\ initial\ MET\ /\ SIL} \times 100\% \quad (1)$$

$$DL = \frac{Weight\ of\ MET\ /\ SIL\ in\ NPs}{Weight\ of\ NPs} \times 100\% \quad (2)$$

2.4. In vitro drug release study

The dialysis technique was applied to evaluate the *in vitro* release of MET and SIL from PLGA-PEG NPs as follows: drug-loaded NPs (25 mg) were dispersed in the phosphate buffer solution (PBS, pH 7.4, 5 ml) and added into a dialysis tube afterward, stirred at 100 rpm and incubated in 37 °C. At designated time intervals, the environmental buffer solution was reconstituted by an equal volume of fresh PBS solution. The concentration of the liberated drugs was assessed by ultraviolet spectrophotometry (Perkin–Elmer, Fremont, CA, USA) at their maximum absorbance wavelengths and calculated by standard curve.

2.5. Cytotoxicity assay

The cytotoxic activity of drugs in free and loaded in PLGA-PEG NPs forms was assessed by the MTT assay 72 h after exposure with drugs. For this assay, 2×10^4 cells/well were cultivated in a 96-well plate and incubated for 24 h at 37 °C in a humidified atmosphere containing 5% CO_2 to allow the cell attachment. Next, the cells were treated with different concentrations of MET and SIL in a constant ratio to one another (250:1) based on their IC50s.

After 72 h of incubation, the cell culture media of all wells was removed and substituted with 200 μl of the phosphate-buffer solution containing 0.5 mg/ml of MTT, and the plates were coated with an aluminum foil and incubated for 4 h at 37 °C. In the following, all content of the wells was eliminated; by adding 200 μl of pure DMSO, 25 μl Sorensen's glycine buffer and incubation for 20 min formed formazan crystals were extracted. Finally, the viability of the cell lines following the respective treatment was evaluated at the formazan maximum absorbance wavelengths (570 nm) using an ELISA-microplate reader (BioTek Power Wave XS) with a reference wavelength of 630 nm. All experiments were performed 3 times.

2.6. Real-time RT-PCR

After 72 h exposure of free and drug-loaded NPs, total cellular RNA was isolated by Trizol reagent (Invitrogen, Carlsbad, CA) in accordance with the manufacturer's procedure. Next, the purity and concentration of the extracted RNA were evaluated via a Nanodrop ND1000 spectrophotometer (OD260/280 ratio). Furthermore, the integrity of isolated RNA was confirmed using agarose gel electrophoresis (1.5% agarose). Complementary DNA (cDNA) was synthesized from RNA applying a First-strand cDNA synthesis kit (Fermentas, Vilnius, Lithuania), based on the manufacturer's protocol. Subsequently, the qPCR technique with the Hot Taq EvaGreen qPCR Mix was applied to assess the hTERT gene expression levels, referring to the manufacturer's instructions. The specific primers that were used for real-time PCR were blasted by the primer-blast on the NCBI website. The Real-time PCR program for incubation of the mixture reaction was as follows; The holding step for 10 min at 95 °C, the denaturation step for 15 s at 95 °C (1 cycle), annealing step for 30 s at 60 °C (40 cycles), extension step for 30 s at 72 °C (40 cycles), and melting step at 65–95 °C (1 cycle). Finally, the relative expression amounts of the hTERT were normalized via the housekeeping gene (GAPDH) and were computed using the 2-ΔΔCT formula.

2.7. Statistical analysis

Graph Pad Prism software (version 6.7) was applied for the statistical analysis of data. Findings with P values ≤ 0.05 were considered to be statistically significant and reported as the mean ± SD (standard deviation). All experiments were accomplished in three replicates. A comparison between the two samples (control and treated) was performed via the two-way analysis of variances (ANOVA).

3. Results and discussion

3.1. Characterization of tri-block copolymer PLGA-b-PEG-b-PLGA

Several different synthetic and natural polymers have been increasingly utilized for nanomedicine applications especially as nanoparticulate drug delivery systems over the past decades [23–25]. Among them, PLGA has been widely investigated for developing devices for controlled delivery of therapeutic molecules with promising outcomes, either alone or in combination with other biomaterials owing to its superior biocompatibility and biodegradability with a board spectrum of erosion times and tunable mechanical features [16,26]. Besides, it was demonstrated that surface functionalization of PLGA NPs with other polymers such as PVA and PEG can significantly improve their biocompatibility, targeting strategy, and blood circulation time [27,28]. In particular, the hydrophilicity of PLGA NPs enhances through PEGylation generating a stealth particle with improved blood circulation half-life and enhanced pharmacokinetics via arresting opsonization and phagocytic uptake [29,30]. Therefore, in this work, we tend to use tri-block copolymer PLGA-*b*-PEG-*b*-PLGA for loading SIL and MET.

The structure of the synthesized biodegradable tri-block copolymer PLGA-*b*-PEG-*b*-PLGA was demonstrated by ^{1}H NMR spectroscopy (Fig. 1). Peaks at 5.19 ppm (a) and 1.56 ppm (d) were corresponded to the protons (–CH–) and methyl protons ($–CH_3$) of the PLA segment, respectively. The peak at 4.82 ppm (b) assigned to the methylene protons ($–CH_2–$) of the PGA segment, and that at 3.65 ppm (c) represented the methylene protons ($–CH_2–$) of PEG [31]. As indicated in Fig. 1, the GPC curve exhibits a unimodal pattern, implying that tri-block copolymer PLGA-*b*-PEG-*b*-PLGA, not a simple physical mixture of PGA, PLA, and PEG, had been successfully synthesized. The polydispersity index (PDI) of the copolymers were only 1.70, and the number average molecular weight, Mn measured by GPC was found to be 31,550. The yield of the synthesized copolymers was 88.5%.

3.2. Characterization of dual drug-loaded NPs

SIL and MET were co-loaded into the copolymer via the water-in-oil-in-water (W/O/W) emulsion method, a common and well-characterized procedure for creating therapeutic molecules-loaded polymeric NPs [32]. In particular, the co-delivery of MET and SIL with different degrees of water solubility was an important challenge in developing a nanocarrier-mediated co-delivery system for their application simultaneously. The double emulsion method uses a two-step process of preparing a water-in-oil (W/O) emulsion for loading biomolecules, pursued by producing W/O/W emulsion in water applying surfactants to construct NPs [33]. Through this process, the encapsulation of both hydrophilic and hydrophobic therapeutic molecules into NPs have been provided. In the current study, the improved W/O/W technique was applied to attain the co-loaded MET/SIL PLGA-PEG NPs.

The amphiphilic PLGA-PEG copolymers should be small enough to avoid the reconnaissance and demolition via the immune systems and extend the drug circulation life span [34]. A zeta potential analyzer with the DLS technique was used to assess the diameter and size distribution of NPs (Fig. 2a and Table 1). As presented in Table 1, drug-free NPs displayed an average particle size of 205 ± 7.23 nm with a uniform size distribution, a polydispersity index (PDI) of 0.169, and zeta potential of −7.2 ± 0.05 mV. Whereas, the average size of MET-NPs and SIL-NPs were bigger than drug-free NPs, inferring the loading of drugs in the core of NPs which lead to an increased diameter. The NPs containing both MET and SIL represented the largest size with a mean hydrodynamic diameter of ~246. The PDI of MET/SIL-loaded NPs was lower than single drug-encapsulated NPs owing to the co-loading of MET and SIL, which lead to forming the well-knit structures of the NPs.

The surface charge of NPs (zeta potential measurement) fundamentally acts as a crucial factor influencing the short- and long-term biostability of NPs and the interaction between NPs and cell membranes

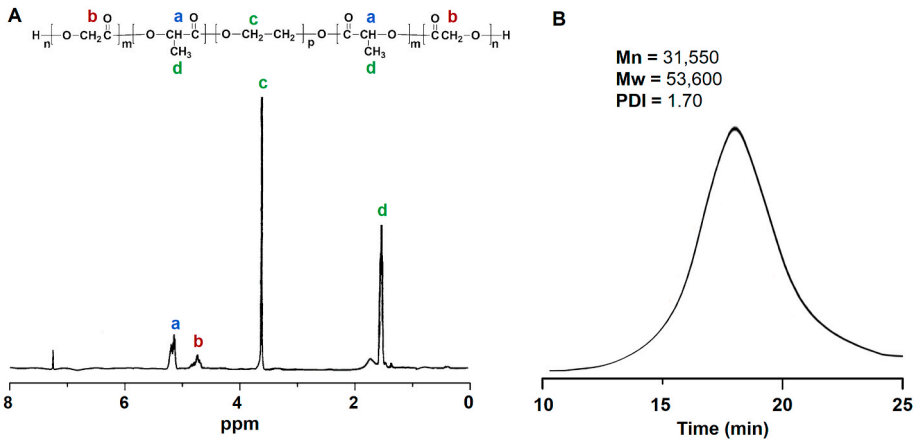

Fig. 1. ^{1}H NMR spectrum (A) and GPC curve (B) of tri-block copolymer PLGA-*b*-PEG-*b*-PLGA.

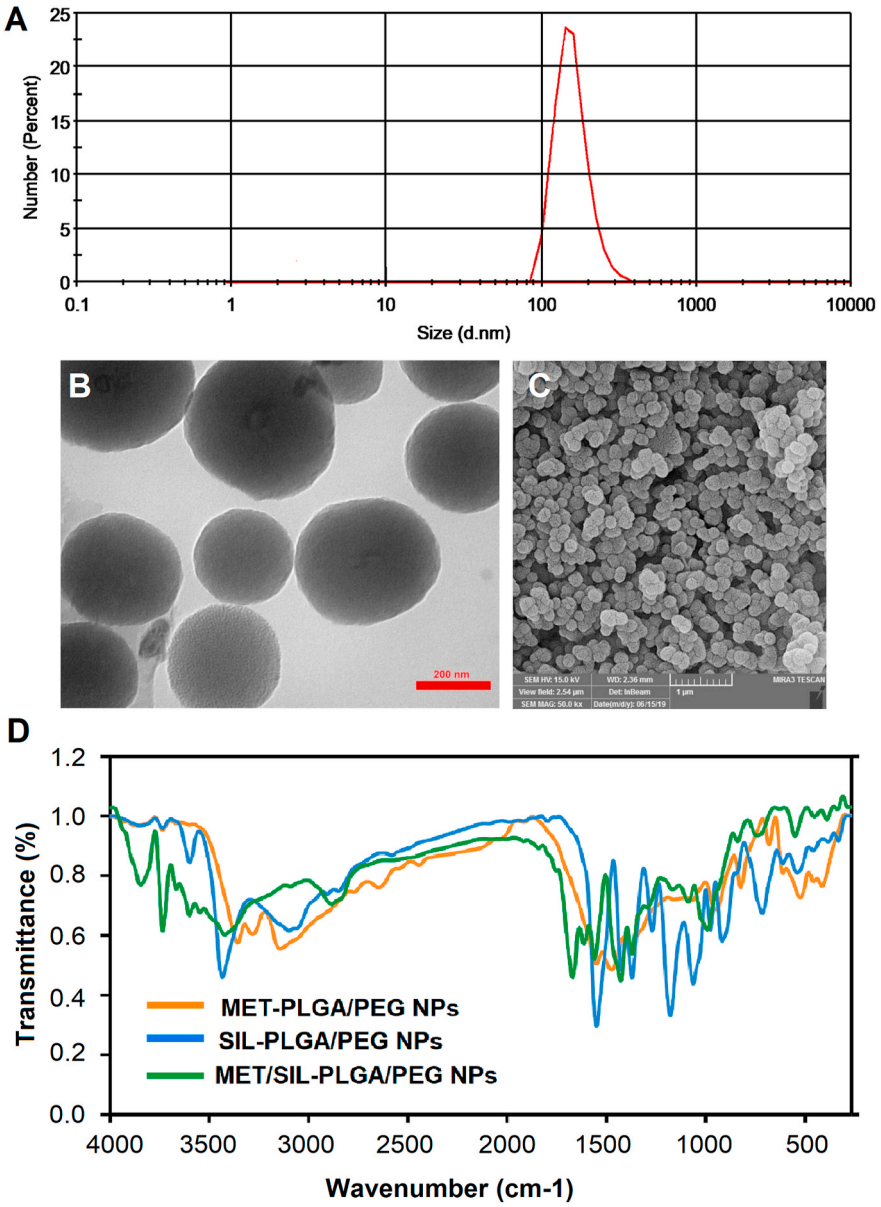

Fig. 2. Size and morphological characterization of NPs. Dynamic light scattering (DLS) histogram (A), Transmission electron microscopy (TEM) image (B), Field emission scanning electron microscopy (FE-SEM) micrograph of MET/SIL-loaded PLGA-PEG NPs, and FT-IR spectra of MET-loaded PLGA-PEG, SIL-loaded PLGA-PEG, and MET/SIL-loaded PLGA-PEG NPs (D).

Table 1
Characterization of PLGA-PEG NPs and drug-loaded NPs using DLS.

Groups	Particle size (nm)	Polydispersity	Zeta potential (mV)
PLGA-PEG NPs	205 ± 7.23	0.169	−7.2 ± 0.05
MET-loaded PLGA-PEG NPs	206 ± 9.37	0.153	−6.1 ± 0.40
SIL-loaded PLGA-PEG NPs	218 ± 8.16	0.129	−6.2 ± 0.35
MET-SIL loaded PLGA-PEG NPs	246 ± 8.43	0.110	−3.8 ± 0.07

[35]. The average surface charge between −7.1 and −3.8 mV was detected for the synthesized NPs (Table 1). The occurrence of deprotonation in free carboxyl groups of PLGA produces a negative charge polymer chain causing the negative values of zeta potential for NPs.

As compared to larger NPs, smaller mean diameter NPs fundamentally have a higher velocity of migration in a known applied electric field and therefore possess higher values of zeta potential, causing augmented stability of NPs in colloidal dispersions [35].

Further investigation on the size as well as the morphology of the NPs was carried out using TEM and FE-SEM (Fig. 2b and c). The representative TEM image indicated that MET/SIL-loaded NPs were distributed uniformly with spherical shapes and a mean diameter of around 220.5 nm. Also, the micrographs obtained from FE-SEM verified the particle size and morphology of the NPs characterized by the TEM.

The modest deviation in the size of the NPs measured through DLS and FE-SEM/TEM has been attributed to the in the surface changes of the samples under the assay conditions employed, so that, the samples are severely dehydrated for FE-SEM and TEM analysis, while for DLS assessment, the NPs must be in the fully hydrated form [36].

It has been reported that the NPs with diameters less than 400 nm are capable to internalize to the cancer cells. Besides, to avid macrophage arresting and guarantee the effective endocytosis into the cancer cells, NPs with high enough size are demanded. Hence, regarding the mentioned physicochemical properties, MET/SIL-loaded PLGA-PEG NPs can be considered promising candidates for internalization into the cancer cells and exerting efficient anticancer effects [36].

FTIR spectroscopy was used to demonstrate the structure of PLGA-PEG NPs and drugs loaded into PLGA-PEG NPs (Fig. 2d). From the infrared spectra of SIL-NPs, the bands at 2885 cm^{-1} owing to C–H stretch of CH, and 3010 cm^{-1} and 2955 cm^{-1} are due to C–H stretch of CH. A sharp band at 1630 cm^{-1} is owing to *C*–O stretch. Absorption at 1186–1089.6 cm^{-1} is assigned to C–O stretch. It was detected that all the characteristic bands of PLGA-PEG and MET are visible in MET-loaded PLGA-PEG NPs IRs. –OH and –NH bands of PLGA-PEG and MET were assigned to the broad peak at 3300-3600 cm^{-1}. The results displayed successful integration and loading of SIL and MET into PLGA-PEG NPs. These findings are in accordance with the results of Amirsaadat et al. and Javidfar et al. [1,37].

It was found that the encapsulation efficiencies of MET and SIL in the prepared dual drug-loaded NPs were 75.15 and 80.5% with a loading capacity of 12.5 ± 2.1 and 10.1 ± 2.2%, respectively. The high entrapment efficiency of SIL compared to MET was assigned to the hydrophobic nature of the molecule.

3.3. In vitro release profiles

To explore the release profile of MET and SIL from the PLGA-PEG NPs, the dialysis membrane technique was applied at pH 7.4. As shown in Fig. 3a, in the first 8 h, an initial rapid release was observed for both the drugs which followed by a sustained discharge over 12 days, and closely 70% and 87% of MET and SIL were liberated within 3 days. The differences in the discharge quantities of MET and SIL from MET/SIL-loaded NPs might be attributed to differences in their hydrophobicity values. These findings were consistent with the release pattern for other drugs from PLGA-PEG NPs reported in previous works [38,39].

It was demonstrated that rapid initial release is assigned to the fraction of the biomolecules which is adsorbed or weakly bound to the high surface area of the NPs rather than to the drugs encapsulated into the polymeric NPs [40].

3.4. MTT assay and synergy analysis

The combined cytotoxic efficiency of MET and SIL co-released from the dual drug-encapsulated PLGA-PEG NPs were investigated on T47D breast cancer cells applying MTT assay. As shown in Fig. 3b, Free single drug and single drug-loaded NPs displayed a dose-dependent cytotoxic effect on T47D cells. The IC_{50} values determined for MET and SIL was relatively high at around 9.61 mM and 38.07 μM, respectively, almost similar to what was previously reported [41,42]. In contrast, the IC_{50} values for MET-NPs and SIL-NPs were measured to be 6.54 mM and 30.99 μM, respectively (Table 2). Particularly, the nanoformulation forms of drugs exerted much higher cytotoxicity toward T47D cells than free drugs after 72 h of treatment, representing that the triggering mechanism for the discharge of the drugs from the endosomes/lysosomes into the cytosol has been extremely effectual. It was found that the co-delivery of MET and SIL was more efficient in arresting the cell proliferation in comparison with the treatment of either drug

Table 2
IC_{50} and combination index (CI_{50}) values for the drug formulations against T47D after 72 h incubation time.

IC_{50}				CI_{50}	
MET (mM)	MET-NPs (mM)	SIL (μM)	SIL-NPs (μM)	MET/SIL	MET/SIL-NPs
9.61	6.54	38.07	30.99	0.91	0.75

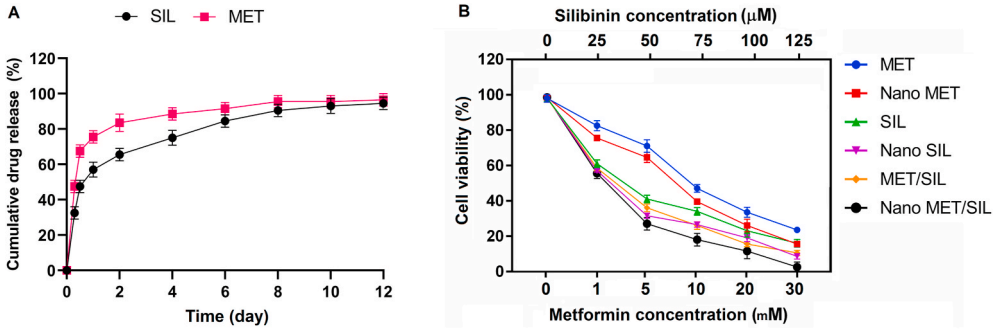

Fig. 3. Drug release patterns of MET and SIL released form MET/SIL-loaded PLGA-PEG NPs in PBS solution at pH 7.4 (A) and cytotoxicity of different concentration of free MET, free SIL, MET-loaded PLGA-PEG NPs, SIL-loaded PLGA-PEG NPs, and MET/SIL-loaded PLGA-PEG NPs on T47D breast cancer cells after 72 h incubation time. The results are presented as mean ± SD (n = 3).

alone, which indicated an interaction between the two therapeutic molecules, which could influence the efficacy of cytotoxicity. Remarkably, the co-delivery of MET and SIL through PLGA-PEG NPs exhibited the highest decrease in cell viability. The increased cytotoxic effects of MET/SIL-loaded PLGA-PEG NPs were might because of the higher cellular uptake, more intracellular concentrations, and efficient interactions of the anticancer agents.

The Chou-Talalay method was applied to analyses the precise nature of this interaction. Using a software, CompySyn, this method provides a combination index (CI) theorem that allows quantitative determination for synergism (CI < 1), additive effect (CI = 1), and antagonism (CI > 1) in drug combinations [43]. The use of Chou-Talalay's CI method in the quantitative determination of drug interaction is increasing steadily during the past two decades. As presented in Table 2, for free MET/SIL and MET/SIL-loaded PLGA-PEG NPs treatments, the CIs value was <1, demonstrating their synergistic inhibitory effects against the viability of T47D cells. Most importantly, the NPs-mediated codelivery of MET and SIL exhibited a remarkable synergistic inhibitory effect and induced higher toxicity on the cells compared to the cocktail free drugs (Table 2).

Some studies have illustrated that SIL in free and combination with MET inhibits the growth and invasion of COLO 205 human cancer cell line through increasing the expression level of PTEN, decreasing the phosphorylation rate of Akt as well as inhibiting the phosphorylation of mTOR by increasing the phosphorylation rate of AMPK, leading to a decline in the metastasis and proliferation of the COLO 205 cell line [44]. Another study has reported the capability of MET and SIL combination to prevent the survival of human cervical cancer cells [12].

3.5. Gene expression analysis

To reveal the anticancer efficiency of the MET and SIL co-loaded PLGA-PEG NPs in the molecular level, the expression of apoptotic genes (Bax, bcl-2, caspase-3, and caspase 9) and hTERT (a protein involved in cancer cell survival) were quantitatively assessed using real-time PCR in the T47D breast cancer cells treated with the IC50s of free and nanoformulation forms of MET and SIL after 72 h incubation time (Fig. 4).

Bcl-2 (anti-apoptotic) and Bax (pro-apoptotic) along with Caspase-3 and 9, components of the cysteine protease family, regulate the mitochondria-mediated apoptosis pathway, and they have a dominant role in the survival of multiple malignancies. Therefore, manipulation on their expression levels is expected to induce the apoptosis process and suppressing cancer cell growth [45].

Besides, unlimited self-renewal is one of the hallmarks of tumor cells and is achieved by telomere maintenance, fundamentally via higher telomerase activation [46]. Transcriptional regulation of hTERT, the catalytic subunit of telomerase is deemed to play a key function in activating telomerase of various tumors [47]. It was proved that the arresting hTERT promotes apoptosis induction in breast cancer cells [48, 49]. Thus, adopting an approach to target and inhibit the apoptosis genes as well as hTERT in breast cancer cells might well be a promising step in breast cancer therapy.

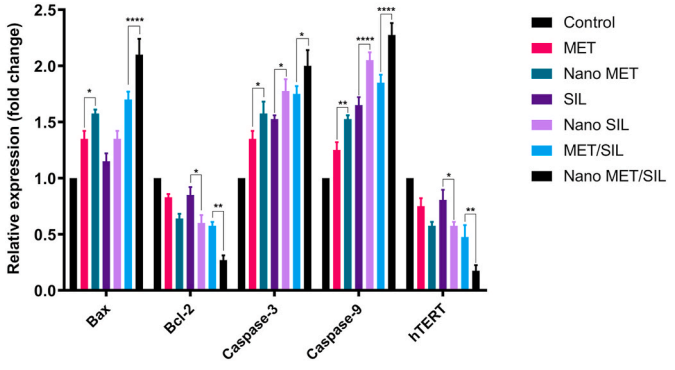

Fig. 4. The expression levels of Bax, Bcl-2, caspase-3, caspase-9 and hTERT in T47D breast cancer cells treated with free MET, free SIL, MET-loaded PLGA-PEG NPs, SIL-loaded PLGA-PEG NPs and MET/SIL-loaded PLGA-PEG NPs after 72 h incubation time. *P < 0.05, ***P < 0.001 and ****P < 0.0001 vs. control was considered significant. Results are mean ± SD (n = 3).

The mechanistic study revealed that treatment with nano-encapsulated forms of MET and SIL exhibited significant down-regulation of hTERT and Bcl-2 as well as upregulation of Bax, caspase-3, and -9 in the cells than the free forms (Fig. 4). The highest alteration in the expression levels of these genes was found in the cells treated with the dual-drug loaded NPs. These results indicated that co-delivery of MET and SIL displayed pronounced effects on apoptosis induction in T47D breast cancer cells, which was consistent with MTT results.

In consistent with our results, several studies demonstrated that MET and SIL alone and or in combined with other chemotherapeutic molecules can alter the expression levels of apoptosis genes and hTERT. Patel and et al. showed that MET was able to induce apoptosis in primary ovarian cancer cells by arresting cell cycle in G0/G1 and S phase, down-regulation of Bcl-2, and up-regulation of Bax [50]. Treatment of COLO 205 human colorectal cancer cells with a combination of MET and SIL induced apoptosis in a dose-dependent manner [44]. In the preliminary study conducted in our group, it was found that MET in combination with SIL exhibits synergistic antiproliferative effects via down-regulating Cyclin D1 and hTERT [42]. Besides, it demonstrated that MET-loaded PLGA-PEG NPs could inhibit the viability of breast and ovarian cancer cells through the reduction of hTERT levels compared to free form [41].

In the present work, we proved that co-releasing of the two natural anticancer agents through a polymeric NPs leads to synergistic cytotoxicity and pro-apoptotic effects against T47D breast cancer cells. Although, testing the efficiency of the dual-drug loaded NPs on other kinds of breast cancer, particularly triple-negative breast cancer cells, as well as on *in vivo* cytotoxicity are crucial to further verify the application of the dual drug-loaded NPs for treatment of breast cancer, which will be of our future interest.

4. Conclusions

In this present work, PLGA-PEG NPs were employed for co-delivery of two natural anticancer agents, MET and SIL against the T47D breast cancer cells. Briefly, drug-loaded NPs were provided with the double emulsion technique, and their characterizations were carried out using FTIR, DLS, TEM, and FE-SEM analysis. According to obtained results, the encapsulation of MET and SIL in PLGA-PEG NPs could effectively inhibit the proliferation of T47D breast cancer cells than their pure forms. Also, it was demonstrated that co-delivery of MET and SIL via PLGA-PEG NPs had a significant synergistic effect in inhibition of the cell viability as well as inducing apoptosis via alteration of the expression levels of Bax, Bcl-2, caspase-3 and 9, and hTERT in T47D breast cancer cells. These results together demonstrate that the co-releasing of MET and SIL via PLGA-PEG NPs were able to enhance the delivery efficiency and might be a promising approach in breast cancer therapy.

Credit author statement

Soumaye Amirsaadat and Davoud Jafari-Gharabaghlou: Methodology, Investigation, Data curation, Original draft preparation.

Sepideh Alijani: Writing- Reviewing and Editing.

Hanieh Mousazadeh: Methodology, Validation, Visualization.

Mehdi Dadashpour: Formal analysis, Software.

Nosratollah Zarghami: Supervision, Conceptualization, Funding acquisition, Reviewing and Editing.

Declaration of competing interest

The authors declare that they have no known competing financial interests or personal relationships that could have appeared to influence the work reported in this paper.

Acknowledgments

We acknowledge financial support from the National Institute for Medical Research Development (Grant No: 982864).

References

[1] S. Sarhadi, S. Sadeghi, F. Nikmanesh, Y. Pilehvar-Soltanahmadi, A. Shahabi, S. F. Aval, N. Zarghami, A systems biology approach provides deeper insights into differentially expressed genes in taxane-anthracycline chemoresistant and non-resistant breast cancers, Asian Pac. J. Cancer Prev. APJCP 18 (10) (2017) 2629.

[2] D. Jafari-Gharabaghlou, Y. Pilehvar-Soltanahmadi, M. Dadashpour, A. Mota, S. Vafajouy-Jamshidi, L. Faramarzi, S. Rasouli, N. Zarghami, Combination of metformin and phenformin synergistically inhibits proliferation and hTERT expression in human breast cancer cells, Irani. J. Basic Med. Sci. 21 (2018) 1167.

[3] R. Naithani, L.C. Huma, R.M. Moriarty, D.L. McCormick, R.G. Mehta, Comprehensive review of cancer chemopreventive agents evaluated in experimental carcinogenesis models and clinical trials, Curr. Med. Chem. 15 (2008) 1044–1071.

[4] Z.J. Maasomi, Y.P. Soltanahmadi, M. Dadashpour, S. Alipour, S. Abolhasani, N. Zarghami, Synergistic anticancer effects of silibinin and chrysin in T47D breast cancer cells, Asian Pac. J. Cancer Prev. APJCP 18 (2017) 1283.

[5] Y. Peng, J. Nie, W. Cheng, G. Liu, D. Zhu, L. Zhang, C. Liang, L. Mei, L. Huang, X. Zeng, A multifunctional nanoplatform for cancer chemo-photothermal synergistic therapy and overcoming multidrug resistance, Biomaterials science 6 (2018) 1084–1098.

[6] A. Alibakhshi, J. Ranjbari, Y. Pilehvar-Soltanahmadi, M. Nasiri, M. Mollazade, N. Zarghami, An update on phytochemicals in molecular target therapy of cancer: potential inhibitory effect on telomerase activity, Curr. Med. Chem. 23 (2016) 2380–2393.

[7] C. Agarwal, R.P. Singh, S. Dhanalakshmi, A.K. Tyagi, M. Tecklenburg, R. A. Sclafani, R. Agarwal, Silibinin upregulates the expression of cyclin-dependent kinase inhibitors and causes cell cycle arrest and apoptosis in human colon carcinoma HT-29 cells, Oncogene 22 (2003) 8271.

[8] P. Tiwari, K. Mishra, Silibinin in cancer therapy: a promising prospect, Cancer Res. Front. 1 (2015) 303–318.

[9] L. Pizzuti, P. Vici, L. Di Lauro, D. Sergi, M. Della Giulia, P. Marchetti, M. Maugeri-Saccà, A. Giordano, M. Barba, Metformin and breast cancer: basic knowledge in clinical context, Canc. Treat Rev. 41 (2015) 441–447.

[10] I. Pernicova, M. Korbonits, Metformin [mdash] mode of action and clinical implications for diabetes and cancer, Nat. Rev. Endocrinol. 10 (2014) 143–156.

[11] S. Ikhlas, M. Ahmad, Metformin: insights into its anticancer potential with special reference to AMPK dependent and independent pathways, Life Sci. 185 (2017) 53–62.

[12] W.-S. Liou, L.-J. Chen, H.-S. Niu, T.-T. Yang, J.-T. Cheng, K.-C. Lin, Herbal product silibinin-induced programmed cell death is enhanced by metformin in cervical cancer cells at the dose without influence on nonmalignant cells, J. Appl. Biomed. 13 (2015) 113–121.

[13] S. Samadzadeh, S. Ghareghomi, H. Mousazadeh, M. Aghababazadeh, Y. Pilehvar-Soltanahmadi, N. Zarghami, An implantable smart hyperthermia nanofiber with switchable, controlled and sustained drug release: possible application in prevention of cancer local recurrence, Mater. Sci. Eng. C (2020) 111384.

[14] S.E. Yazdi Rouholamini, S. Moghassemi, Z. Maharat, A. Hakamivala, S. Kashanian, K. Omidfar, Effect of silibinin-loaded nano-niosomal coated with trimethyl chitosan on miRNAs expression in 2D and 3D models of T47D breast cancer cell line, Artif. Cells Nanomed. Biotechnol. (2017) 1–12.

[15] Y. Dang, J. Guan, Nanoparticle-based drug delivery systems for cancer therapy, Smart Materials in Medicine (2020).

[16] F. Mohammadian, Y. Pilehvar-Soltanahmadi, M. Mofarrah, M. Dastani-Habashi, N. Zarghami, Down regulation of miR-18a, miR-21 and miR-221 genes in gastric cancer cell line by chrysin-loaded PLGA-PEG nanoparticles, Artif. Cells Nanomed. Biotechnol. 44 (2016) 1972–1978.

[17] M. Montazeri, M. Sadeghizadeh, Y. Pilehvar-Soltanahmadi, F. Zarghami, S. Khodi, M. Mohaghegh, H. Sadeghzadeh, N. Zarghami, Dendrosomal curcumin nanoformulation modulate apoptosis-related genes and protein expression in hepatocarcinoma cell lines, Int. J. Pharm. 509 (2016) 244–254.

[18] N. Naseri, E. Ajorlou, F. Asghari, Y. Pilehvar-Soltanahmadi, An update on nanoparticle-based contrast agents in medical imaging, Artif. Cells Nanomed. Biotechnol. 46 (2018) 1111–1121.

[19] M. Mehrabi, N.M. Dounighi, S.M. Rezayat Sorkhabadi, D. Doroud, A. Amani, M. Khoobi, S. Ajdary, Y. Pilehvar-Soltanahmadi, Development and physicochemical, toxicity and immunogenicity assessments of recombinant hepatitis B surface antigen (rHBsAg) entrapped in chitosan and mannosylated chitosan nanoparticles: as a novel vaccine delivery system and adjuvant, Artif. Cells Nanomed. Biotechnol. 46 (2018) 230–240.

[20] F. Mohammadian, A. Abhari, H. Dariushnejad, A. Nikanfar, Y. Pilehvar-Soltanahmadi, N. Zarghami, Effects of chrysin-PLGA-PEG nanoparticles on proliferation and gene expression of miRNAs in gastric cancer cell line, Iran. J. Cancer Prev. 9 (2016).

[21] R. Farajzadeh, Y. Pilehvar-Soltanahmadi, M. Dadashpour, S. Javidfar, J. Lotfi-Attari, H. Sadeghzadeh, V. Shafiei-Irannejad, N. Zarghami, Nano-encapsulated metformin-curcumin in PLGA/PEG inhibits synergistically growth and hTERT gene expression in human breast cancer cells, Artif. Cells Nanomed. Biotechnol. (2017) 1–9.

[22] K. Snima, R.S. Nair, S.V. Nair, C.R. Kamath, V.-K. Lakshmanan, Combination of anti-diabetic drug metformin and boswellic acid nanoparticles: a novel strategy for pancreatic cancer therapy, J. Biomed. Nanotechnol. 11 (2015) 93–104.

[23] K. Nejati-Koshki, Y. Mortazavi, Y. Pilehvar-Soltanahmadi, S. Sheoran, N. Zarghami, An update on application of nanotechnology and stem cells in spinal cord injury regeneration, Biomed. Pharmacother. 90 (2017) 85–92.

[24] M. Dadashpour, A. Firouzi-Amandi, M. Pourhassan-Moghaddam, M.J. Maleki, N. Soozangar, F. Jeddi, M. Nouri, N. Zarghami, Y. Pilehvar-Soltanahmadi, Biomimetic synthesis of silver nanoparticles using Matricaria chamomilla extract and their potential anticancer activity against human lung cancer cells, Mater. Sci. Eng. C 92 (2018) 902–912.

[25] M. Montazeri, Y. Pilehvar-Soltanahmadi, M. Mohaghegh, A. Panahi, S. Khodi, N. Zarghami, M. Sadeghizadeh, Antiproliferative and apoptotic effect of dendrosomal curcumin nanoformulation in P53 mutant and wide-type cancer cell lines, Anti Canc. Agents Med. Chem. 17 (2017) 662–673.

[26] X. Zeng, W. Tao, L. Mei, L. Huang, C. Tan, S.-S. Feng, Cholic acid-functionalized nanoparticles of star-shaped PLGA-vitamin E TPGS copolymer for docetaxel delivery to cervical cancer, Biomaterials 34 (2013) 6058–6067.

[27] W. Cheng, J. Nie, N. Gao, G. Liu, W. Tao, X. Xiao, L. Jiang, Z. Liu, X. Zeng, L. Mei, A multifunctional nanoplatform against multidrug resistant cancer: merging the best of targeted chemo/gene/photothermal therapy, Adv. Funct. Mater. 27 (2017) 1704135.

[28] A. Firouzi-Amandi, M. Dadashpour, M. Nouri, N. Zarghami, H. Serati-Nouri, D. Jafari-Gharabaghlou, B.H. Karzar, H. Mellatyar, L. Aghebati-Maleki, Z. Babaloo, Chrysin-nanoencapsulated PLGA-PEG for macrophage repolarization: possible application in tissue regeneration, Biomed. Pharmacother. 105 (2018) 773–780.

[29] X. Zeng, G. Liu, W. Tao, Y. Ma, X. Zhang, F. He, J. Pan, L. Mei, G. Pan, A drug-self-gated mesoporous antitumor nanoplatform based on pH-sensitive dynamic covalent bond, Adv. Funct. Mater. 27 (2017) 1605985.

[30] W. Cheng, X. Zeng, H. Chen, Z. Li, W. Zeng, L. Mei, Y. Zhao, Versatile polydopamine platforms: synthesis and promising applications for surface modification and advanced nanomedicine, ACS Nano 13 (2019) 8537–8565.

[31] N. Gao, Z. Chen, X. Xiao, C. Ruan, L. Mei, Z. Liu, X. Zeng, Surface modification of paclitaxel-loaded tri-block copolymer PLGA-b-PEG-b-PLGA nanoparticles with protamine for liver cancer therapy, J. Nanoparticle Res. 17 (2015) 347.

[32] F. Mohammadian, A. Abhari, H. Dariushnejad, F. Zarghami, A. Nikanfar, Y. Pilehvar-Soltanahmadi, N. Zarghami, Upregulation of Mir-34a in AGS gastric cancer cells by a PLGA-PEG-PLGA chrysin nano formulation, Asian Pac. J. Cancer Prev. APJCP 16 (2016) 8259–8263.

[33] F. Mohammadian, Y. Pilehvar-Soltanahmadi, F. Zarghami, A. Akbarzadeh, N. Zarghami, Upregulation of miR-9 and Let-7a by nanoencapsulated chrysin in gastric cancer cells, Artif. Cells Nanomed. Biotechnol. 45 (2017) 1201–1206.

[34] H. Sadeghzadeh, Y. Pilehvar-Soltanahmadi, A. Akbarzadeh, H. Dariushnejad, F. Sanjarian, N. Zarghami, The effects of nanoencapsulated curcumin-Fe3O4 on proliferation and hTERT gene expression in lung cancer cells, Anti Canc. Agents Med. Chem. 17 (2017) 1363–1373.

[35] F. Tavakoli, R. Jahanban-Esfahlan, K. Seidi, M. Jabbari, R. Behzadi, Y. Pilehvar-Soltanahmadi, N. Zarghami, Effects of nano-encapsulated curcumin-chrysin on telomerase, MMPs and TIMPs gene expression in mouse B16F10 melanoma tumour model, Artificial cells, nanomedicine, and biotechnology 46 (2018) 75–86.

[36] J. Lotfi-Attari, Y. Pilehvar-Soltanahmadi, M. Dadashpour, S. Alipour, R. Farajzadeh, S. Javidfar, N. Zarghami, Co-delivery of curcumin and chrysin by polymeric nanoparticles inhibit synergistically growth and hTERT gene expression in human colorectal cancer cells, Nutr. Canc. 69 (2017) 1290–1299.

[37] S. Amirsaadat, Y. Pilehvar-Soltanahmadi, F. Zarghami, S. Alipour, Z. Ebrahimnezhad, N. Zarghami, Silibinin-loaded magnetic nanoparticles inhibit hTERT gene expression and proliferation of lung cancer cells, Artif. Cells Nanomed. Biotechnol. 45 (2017) 1649–1656.

[38] S. Gholizadeh, J.A. Kamps, W.E. Hennink, R.J. Kok, PLGA-PEG nanoparticles for targeted delivery of the mTOR/PI3kinase inhibitor dactolisib to inflamed endothelium, Int. J. Pharm. 548 (2018) 747–758.

[39] S. Moffatt, R. Cristiano, R. Boyle, Combined formulation of Doxorubicin-Arg-Gly-Asp (RGD) and modified PEGylated PLGA-encapsulated nanocarrier improves anti-tumor activity, in: 2012 IEEE International Conference on Bioinformatics and Biomedicine Workshops, IEEE, 2012, pp. 903–909.

[40] S. Mashayekhi, S. Rasoulpoor, S. Shabani, N. Esmaeilizadeh, H. Serati-Nouri, R. Sheervalilou, Y. Pilehvar-Soltanahmadi, Curcumin-loaded mesoporous silica nanoparticles/nanofiber composites for supporting long-term proliferation and stemness preservation of adipose-derived stem cells, Int. J. Pharm. 587 (2020) 119656.

[41] S. Javidfar, Y. Pilehvar-Soltanahmadi, R. Farajzadeh, J. Lotfi-Attari, V. Shafiei-Irannejad, M. Hashemi, N. Zarghami, The inhibitory effects of nano-encapsulated metformin on growth and hTERT expression in breast cancer cells, J. Drug Deliv. Sci. Technol. 43 (2018) 19–26.

[42] M. Chatran, Y. Pilehvar-Soltanahmadi, M. Dadashpour, L. Faramarzi, S. Rasouli, D. Jafari-Gharabaghlou, N. Asbaghi, N. Zarghami, Synergistic anti-proliferative

effects of metformin and silibinin combination on T47D breast cancer cells via hTERT and cyclin D1 inhibition, Drug Res. 68 (2018) 710–716.
[43] T.-C. Chou, Drug combination studies and their synergy quantification using the Chou-Talalay method, Canc. Res. 70 (2010) 440–446.
[44] C.-C. Tsai, T.-W. Chuang, L.-J. Chen, H.-S. Niu, K.-M. Chung, J.-T. Cheng, K.-C. Lin, Increase in apoptosis by combination of metformin with silibinin in human colorectal cancer cells, World journal of gastroenterology, WJG 21 (2015) 4169.
[45] B.A. Carneiro, W.S. El-Deiry, Targeting apoptosis in cancer therapy, Nat. Rev. Clin. Oncol. (2020) 1–23.
[46] A. Zavari-Nematabad, M. Alizadeh-Ghodsi, H. Hamishehkar, E. Alipour, Y. Pilehvar-Soltanahmadi, N. Zarghami, Development of quantum-dot-encapsulated liposome-based optical nanobiosensor for detection of telomerase activity without target amplification, Anal. Bioanal. Chem. 409 (2017) 1301–1310.
[47] S. Pirmoradi, E. Fathi, R. Farahzadi, Y. Pilehvar-Soltanahmadi, N. Zarghami, Curcumin affects adipose tissue-derived mesenchymal stem cell aging through TERT gene expression, Drug Research 68 (2018) 213–221.
[48] S. Talaei, H. Mellatyar, Y. Pilehvar-Soltanahmadi, A. Asadi, A. Akbarzadeh, N. Zarghami, 17-Allylamino-17-demethoxygeldanamycin loaded PCL/PEG nanofibrous scaffold for effective growth inhibition of T47D breast cancer cells, J. Drug Deliv. Sci. Technol. 49 (2019) 162–168.
[49] S. Rasouli, M. Montazeri, S. Mashayekhi, S. Sadeghi-Soureh, M. Dadashpour, H. Mousazadeh, A. Nobakht, N. Zarghami, Y. Pilehvar-Soltanahmadi, Synergistic anticancer effects of electrospun nanofiber-mediated codelivery of Curcumin and Chrysin: possible application in prevention of breast cancer local recurrence, J. Drug Deliv. Sci. Technol. 55 (2020) 101402.
[50] S. Patel, L. Kumar, N. Singh, Metformin and epithelial ovarian cancer therapeutics, Cell. Oncol. 38 (2015) 365–375.